

## High pressure neutron diffraction investigation of CuO

This article has been downloaded from IOPscience. Please scroll down to see the full text article.

2005 J. Phys.: Condens. Matter 17 S3057

(<http://iopscience.iop.org/0953-8984/17/40/008>)

View [the table of contents for this issue](#), or go to the [journal homepage](#) for more

Download details:

IP Address: 129.252.86.83

The article was downloaded on 28/05/2010 at 06:00

Please note that [terms and conditions apply](#).

# High pressure neutron diffraction investigation of CuO

T Chatterji<sup>1</sup>, P J Brown<sup>1,2</sup> and J B Forsyth<sup>3</sup>

<sup>1</sup> Institut Laue-Langevin, BP156 F 38042 Cedex, France

<sup>2</sup> Department of Physics, Loughborough University, Loughborough LE11 3TU, UK

<sup>3</sup> ISIS Facility, Rutherford Appleton Laboratory, Chilton, Didcot, UK

Received 8 July 2005

Published 23 September 2005

Online at [stacks.iop.org/JPhysCM/17/S3057](http://stacks.iop.org/JPhysCM/17/S3057)

## Abstract

The dependence of the magnetic structure of CuO on hydrostatic pressure up to 18 kbar has been studied by means of neutron diffraction at low temperatures. The pressure dependences of both the Néel temperature  $T_N$  and the incommensurate–commensurate lock-in transition temperature  $T_L$  have been determined. The Néel temperature, which is 230 K at ambient pressure, increases to  $T_N = 235$  K at  $P = 18$  kbar, whereas the lock-in transition temperature, which is 213 K at ambient pressure, decreases continuously to  $T_L = 207$  K at  $P = 18$  kbar. Since hydrostatic pressure increases the stability range of the incommensurate phase, it is likely that at very high pressures the incommensurate phase would be the only stable ordered magnetic phase of CuO and the commensurate antiferromagnetic phase would be completely suppressed.

(Some figures in this article are in colour only in the electronic version)

## 1. Introduction

The magnetic properties of cupric oxide CuO have been studied intensively due to their similarity to those of the undoped parent compounds of the high  $T_c$  superconductors. Unlike those of the latter compounds, the structure of CuO does not contain CuO<sub>2</sub> layers but the coordination of copper with oxygen is approximately square planar. The magnetic susceptibility shows only minute anomalies at the Néel temperature and continues to increase above  $T_N$  showing a broad maximum around 600 K and finally decreases at higher temperatures [1, 2]. Calorimetric studies [3, 4] show that more than 70% of the magnetic entropy is associated with the short range order and  $\Delta S_m$  only approaches the value expected for a  $S = \frac{1}{2}$  system around 1000 K. The above results suggest quasi-low dimensional magnetic behaviour. Our inelastic and quasielastic neutron scattering investigations [5, 6] did indeed confirm that CuO has a quasi-one-dimensional magnetic character. Neutron diffraction investigations [7] established that CuO orders at  $T_N = 230$  K to an incommensurate helimagnetic phase with the wavevector  $\mathbf{k} = (0.506, 0, -0.483)$  which is temperature independent within experimental resolution. At  $T_L = 213$  K this helimagnetic phase locks

into a commensurate antiferromagnetic phase with the wavevector  $\mathbf{k} = (\frac{1}{2}, 0, -\frac{1}{2})$ . The magnetic structures of the commensurate and the incommensurate phases of CuO have been investigated in detail using both unpolarized and polarized neutron diffraction [8]. In the commensurate antiferromagnetic phase the magnetic moments are parallel to the monoclinic  $b$  axis of the crystal. The magnetic structure of the incommensurate phase is helical and its elliptical modulation envelope has one axis parallel to [010] and the other in the  $a$ - $c$  plane, making an angle of  $28.2^\circ \pm 0.8^\circ$  to [001] in the obtuse  $\beta$  angle. The envelope is almost circular, the ratio of the  $b$  to the  $a$ - $c$  component is  $1.03 \pm 0.01$  and the normal to the plane of the moments is inclined at  $17.0^\circ \pm 0.5^\circ$  to the wavevector.

## 2. Experimental details

High pressure neutron diffraction experiments were done in normal beam geometry on the diffractometer D15 which is equipped with a tilting detector. Monochromatic neutrons of about 1.72 Å were used for the present investigation. A prism shaped CuO single crystal with linear dimensions of about 2 mm was mounted with its  $b$  axis parallel to the cylindrical axis of the clamp high pressure cell. The pressure applied was determined from the lattice spacing of a small NaCl single crystal placed on top of the CuO crystal. The pressure transmitting medium was deuterated propanol. Please note that although deuterated propanol freezes at the relevant temperature and pressure of our experiment, the solid propanol is a soft molecular solid and still serves as an excellent pressure transmitting medium in the relevant pressure range. So the pressure generated during our measurements is at least quasi-hydrostatic. The clamp pressure cell was fixed to the sample stick of a standard  $^4\text{He}$  cryostat. Two different sized clamps were used: the smaller one generated pressures up to about 10 kbar whereas the larger one could generate pressures up to about 20 kbar.

## 3. Results and discussion

Figure 1 shows the temperature variation of the intensities of the  $\frac{1}{2}, 0, -\frac{1}{2}$  and 0.506, 0, -0.483 reflections corresponding respectively to the commensurate and incommensurate phases of CuO close to the ordering temperatures  $T_N$  and  $T_L$  at ambient pressure and also at  $P = 18$  kbar. The intensity of the  $\frac{1}{2}, 0, -\frac{1}{2}$  reflection decreases abruptly with temperature at  $T_L$  whereas that of the 0.506, 0, -0.483 reflection grows abruptly at about the same temperature. The intensity corresponding to the incommensurate phase goes through a maximum and then decreases continuously and finally becomes zero at  $T_N$ . The temperature variation of these intensities was also measured at several intermediate pressures. The intensity in arbitrary units plotted in figure 1 is the integrated intensity after subtracting the background. The background was rather large due to the scattering from the high pressure cell and its measurement was difficult for weak intensities close to the transition temperatures. The subtraction of the background therefore led to some negative intensities. The lock-in transition temperature could be determined relatively easily from the temperature dependence of the  $\frac{1}{2}, 0, -\frac{1}{2}$  and 0.506, 0, -0.483 reflections, but the determination of  $T_N$  was much less precise. The resulting pressure-temperature ( $P$ - $T$ ) phase diagram of CuO is shown in figure 2.

The Néel temperature increases from  $T_N = 230$  K at ambient pressure to  $T_N = 235$  K at  $P = 18$  kbar, whereas the lock-in transition temperature decreases continuously from  $T_L = 213$  K at ambient pressure to  $T_L = 207$  K at  $P = 18$  kbar, the highest pressure attained during the investigation. Hydrostatic pressure increases the stability range of the incommensurate phase and it is possible that at very high pressures the commensurate

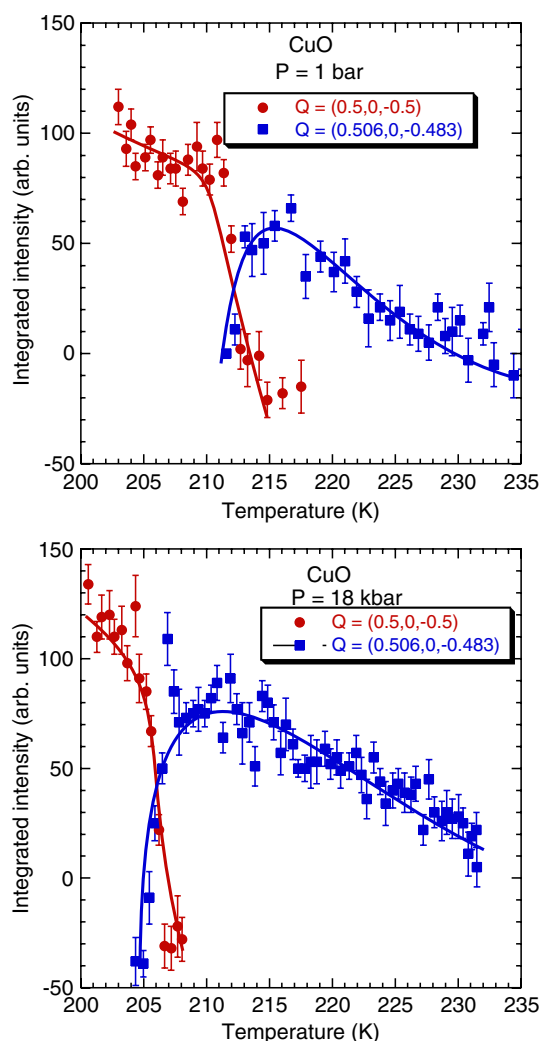


**Figure 1.** Temperature variation of the intensities of the  $\frac{1}{2}, 0, -\frac{1}{2}$  and  $0.506, 0, -0.483$  reflections corresponding to the commensurate and incommensurate phases of CuO as a function of temperature close to the ordering temperatures  $T_N$  and  $T_L$  at ambient pressure and also at  $P = 18$  kbar.

antiferromagnetic phase would be completely suppressed and the incommensurate phase would be the only stable ordered magnetic phase of CuO.

The principal superexchange path in the crystal structure of CuO is through the zigzag Cu–O–Cu chains parallel to  $[1, 0, 1]$ . The Cu–O–Cu bond angle  $\theta_{[10\bar{1}]}$  in these chains is about  $145^\circ$  and this is the highest Cu–O–Cu bond angle in the structure. The next highest Cu–O–Cu bond angle  $\theta_{[101]} = 109^\circ$  occurs in Cu–O–Cu chains along the  $[1, 0, 1]$  direction. All other Cu–O–Cu bond angles are smaller than this. In the undoped parent compounds of the high  $T_c$  superconductors the strength of antiferromagnetic exchange interaction is known to be correlated with the Cu–O–Cu bond angle  $\theta$  although it was found to be uncorrelated with the Cu–O bond lengths [9]. Figure 3 shows the dependence of the superexchange interaction

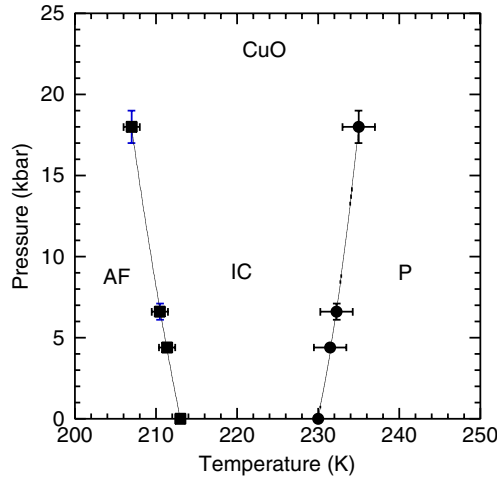


**Figure 2.** Pressure–temperature ( $P$ – $T$ ) phase diagram of CuO.

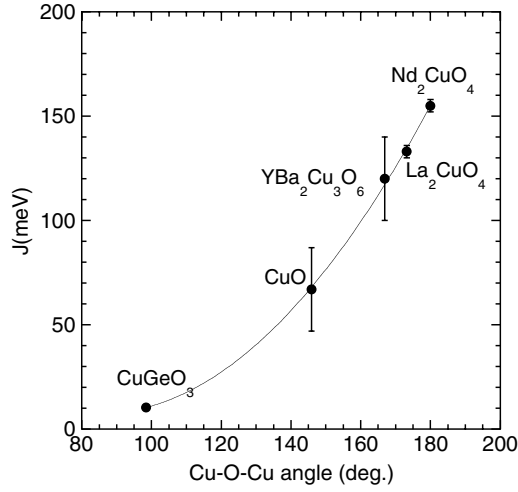


**Figure 3.** The superexchange interaction  $J$  determined from inelastic neutron scattering investigations plotted against the Cu–O–Cu bond angle for several cuprate materials. The continuous curve is a least squares fit of the data points to a second-order polynomial.

$J$  on the Cu–O–Cu bond angle  $\theta$  for several cuprate materials. The same dependence can be used to estimate the relative strengths of exchange interactions along the different Cu–O–Cu bond directions in CuO for which  $\theta$  varies from  $95^\circ$  to  $145^\circ$ . We estimate  $J_1$  along  $[1, 0, \bar{1}]$  to be about 77 meV compared to  $J_2$  along  $[1, 0, 1]$  of about 15 meV, giving a ratio  $J_2/J_1 \approx 0.2$ . This explains the quasi-one-dimensional magnetic property of CuO and is in agreement with the results of specific heat [1, 3], inelastic [6, 10] and quasielastic [5] neutron scattering investigations.

The pressure dependence of the crystal structure of CuO has been investigated by Ehrenberg *et al* [11] and Forsyth and Hull [12] and we have used their data to calculate the Cu–O–Cu bond angles  $\theta_{[10\bar{1}]}$  and  $\theta_{[101]}$  at different pressures; these are shown in figure 4. We note that the angle  $\theta_{[10\bar{1}]}$  increases continuously with pressure whereas  $\theta_{[101]}$  decreases. The

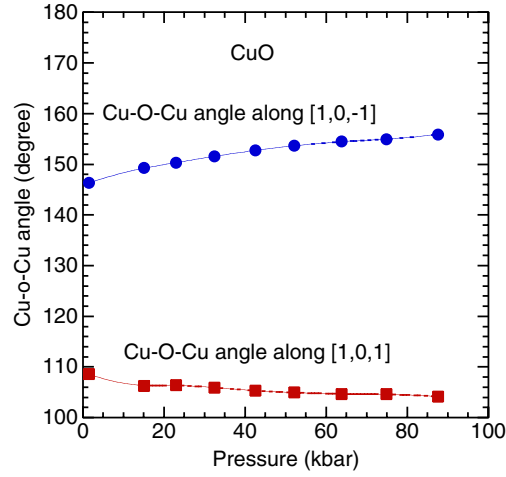


**Figure 4.** Pressure variation of the Cu–O–Cu bond angle  $\theta_{[1,0,\bar{1}]}$  along  $[1, 0, \bar{1}]$  and the bond angle  $\theta_{[1,0,1]}$  along  $[101]$  directions in CuO. The angles have been calculated by using the high pressure structural parameters of Ehrenberg *et al* (filled circles and squares) [11].

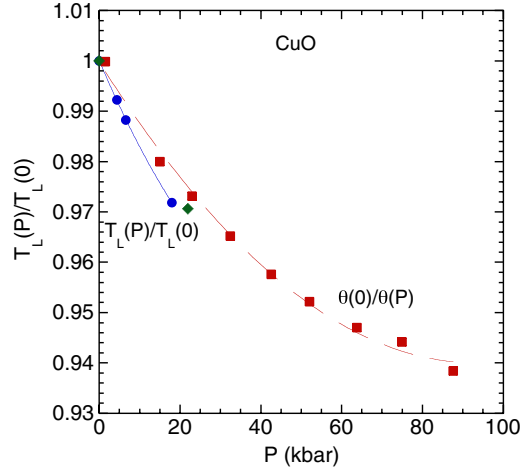


**Figure 5.** Pressure variation of the normalized lock-in transition temperature  $T_L(P)/T_L(0)$  (circles) and the normalized Cu–O–Cu bond angle  $\theta(0)/\theta(P)$  along the  $[1, 0, \bar{1}]$  direction in CuO. The squares and diamonds are  $\theta(0)/\theta(P)$  calculated by using the high pressure structural parameters of Ehrenberg *et al* [11] and Forsyth and Hull [12], respectively.

dominant antiferromagnetic exchange interaction  $J_1$  is associated with  $\theta_{[10\bar{1}]}$  and the relative stabilities of the commensurate and the incommensurate magnetic phases of CuO should therefore be sensitive to this bond angle. To demonstrate this we have plotted in figure 5 the pressure dependence of the normalized lock-in transition temperature  $T_L(P)/T_L(0)$  along with  $\theta(0)/\theta(P)$ , the inverse of the normalized Cu–O–Cu bond angle along  $[1, 0, \bar{1}]$ . Both  $T_L(P)/T_L(0)$  and  $\theta(0)/\theta(P)$  decrease with increasing pressure, which is consistent with a decrease in the dominant antiferromagnetic exchange coupling constant.

In conclusion we have investigated the pressure–temperature ( $P$ – $T$ ) phase diagram of CuO up to 18 kbar and have determined the stabilities of the antiferromagnetic, incommensurate

and the paramagnetic phases. We have discussed the temperature dependence of the lock-in transition in terms of the Cu–O–Cu bond angle along  $[1, 0, \bar{1}]$ .

## References

- [1] O’Keffe M and Stone F S 1962 *J. Phys. Chem. Solids* **23** 261
- [2] Köbler U and Chattopadhyay T 1991 *Z. Phys. B* **82** 383
- [3] Gmelin E, Köbler U, Brill W, Chattopadhyay T and Sastry S 1991 *Bull. Mater. Sci.* **14** 177
- [4] Loram J W, Mirza K A, Joyce C and Osborne J 1989 *Europhys. Lett.* **8** 263
- [5] Chattopadhyay T, McIntyre G J, Vettier C, Brown P J and Forsyth J B 1992 *Physica B* **180/181** 420
- [6] Chattopadhyay T, McIntyre G J, Brown P J and Forsyth J B 1990 *Physica C* **170** 371
- [7] Brown P J, Forsyth J B and Wanklyn B M 1988 *J. Phys. C: Solid State Phys.* **21** 2917
- [8] Brown P J, Chattopadhyay T, Forsyth J B, Nunez V and Tasset F 1991 *J. Phys.: Condens. Matter* **3** 4281
- [9] Shimizu T, Matsumoto T, Goto A and Chandrasekhar Rao T V 2003 *Phys. Rev. B* **68** 224433
- [10] Ain M, Reichardt W, Hennion B, Pepy G and Wanklyn B M 1989 *Physica C* **170** 371
- [11] Eherenberg H, McAllister J A, Marshall W G and Attfield A P 1999 *J. Phys.: Condens. Matter* **11** 6501
- [12] Forsyth J B and Hull S 1991 *J. Phys.: Condens. Matter* **3** 5257